

## Computation of the surface electron-energy-loss spectrum in specular geometry for an arbitrary plane-stratified medium

Ph. Lambin<sup>1</sup>, J.-P. Vigneron and A.A. Lucas

*Institute for Studies in Interface Sciences, Facultés Universitaires Notre-Dame de la Paix,  
Rue de Bruxelles 61, 5000 Namur, Belgium*

Received 22 April 1990

In recent years, high-resolution electron-energy-loss spectroscopy (EELS) has been successfully applied to the study of vibrational properties of surfaces and interfaces of materials having a layered structure. At the same time the theory of long-wavelength electromagnetic properties of surfaces and interfaces and their role in the inelastic scattering processes of electrons at the surface has also developed to a point where detailed quantitative comparisons between experimental and theoretical vibrational spectra can now be made routinely. The computer program described here allows to calculate the EELS spectrum of a large variety of target materials, going from a homogeneous thick substrate to periodic superlattices or any arbitrary stacking of layers.

### PROGRAM SUMMARY

*Title of program:* HREELS of multilayers

*Catalogue number:* ABTI

*Program obtainable from:* CPC Program Library, Queens University of Belfast, N. Ireland (see application form in this issue)

*Computer:* IBM 9377/90; *Installation:* Scientific Computing Facility (SCF), Facultés Universitaires Notre-Dame de la Paix, 5000 Namur, Belgium

*Operating system:* VM/SP Rel 5

*Programming language used:* FORTRAN 77

*High speed storage required:* 65 Kwords

*No. of bits in a word:* 32 and 64

*No. of lines in combined program and test deck:* 1553

*Keywords:* surface analysis, surface and interface phonons, electron-energy-loss spectroscopy, HREELS, thin films, heterostructure, superlattice

<sup>1</sup> Research Associate at the National Fund for Scientific Research of Belgium.

### *Nature of the physical problem*

This computer program allows to calculate the electron-energy-loss spectrum of an arbitrary plane-stratified medium for low-energy electrons specularly reflected at the surface of the target. A dielectric approximation is used to characterize the response of the target material to the long-ranged Coulomb field of the impinging electrons. Periodic superlattices can be considered as well as any arbitrary stacking of layers onto a thick substrate [1]. In the later case, the substrate is allowed to be an anisotropic, uniaxial crystal having its axis perpendicular to the free surface of the system. Temperature effects are included according to Bose–Einstein statistics for the long-wavelength vibrations excited at the surface or interfaces by the electrons [2].

### *Method of solution*

The EELS spectrum is computed in two sequential steps performed by two programs called EELS and BOSON. The single-scattering, classical loss spectrum of the target is first computed (program EELS) for an electron traveling along a specularly reflected trajectory, with the possibility of taking into account the acceleration of the electron by the image force. The full EELS spectrum, which includes multiple-scattering events for an arbitrary temperature of the target, is next obtained through a suitable thermodynamic average of the quantized surface excitations (program BOSON), while keeping the classical nature of the impinging electrons. The computed EELS spectrum is convoluted with a model of the

instrumental response of the spectrometer so as to simulate limitations in the experimental energy resolution.

#### *Restrictions on the complexity of the problem*

Only dipolar inelastic-scatterings of the reflected electrons are considered. Possible variations of the surface reflection coefficient with the electron energy are not considered here as all inelastic spectra are normalized to unity. All the layers that compose the target are assumed to be made of materials having isotropic dielectric functions, except for a possible thick substrate on which the layers are stacked, which can be an uniaxial crystal.

## LONG WRITE-UP

### 1. Introduction

Since the first observations at high resolution of electron-energy-loss processes taking place at the surface of a clean crystal [1], the present understanding of the inelastic scattering of electrons at the surface of a target material by long-wavelength phonons is very advanced. A continuous refinement of the original semi-classical theory of electron-energy-loss spectroscopy (EELS) of surfaces [2] has lead us to a point where we now have a fully quantitative theory for both the line position and the line shape of specular (or Bragg) EELS spectra [3]. On the experimental side, the major result of a longstanding improvement of the technique is the demonstration that high-resolution EELS now constitutes an alternative method to optical spectroscopy – although with a still poorer resolution – for obtaining the frequency-dependent dielectric function of the target material [4]. Moreover, the surface sensitivity of EELS in specular geometry permits the dielectric characterization of the first few hundred Angströms under the free, assumed clean surface: a definitive asset for investigating surface non-homogeneities [5] or for the study of interfacial materials of current interest [6].

The interpretation of experimental data may benefit from detailed comparisons with theoretical predictions allowing fine adjustments of the various parameters (oscillator parameters, layer thickness, composition profile,...) that control the

#### *Typical running time*

The time for the test run on the IBM 9377 is 40 s.

#### *References*

- [1] Ph. Lambin, J.-V. Vigneron and A.A. Lucas, Phys. Rev. B 32 (1985) 8203.
- [2] A.A. Lucas, J.-P. Vigneron, Ph. Lambin, P.A. Thiry, M. Liehr, J.-J. Pireaux and R. Caudano, Int. J. Quantum Chem.: Quantum Chem. Symp. 19 (1986) 687.

surface dielectric response of the target system. More informations about the structure [7] or the composition [8] of the material under investigation is gained from such comparisons and it is the aim of the present paper to propose a computer program permitting to do so.

In this paper, we describe a program for computing the EELS spectrum in specular geometry for an arbitrary plane-stratified medium, i.e. a system in which the composition is a histogram-like function of the coordinate  $z$  perpendicular to the free surface. This class of systems includes e.g. artificial heterostructures obtained by deposition of one or several layers onto a crystalline substrate in well-controlled conditions (composition, layer thickness...) such as realized in molecular beam epitaxy. As the wavelength of the vibrations excited in specular EELS are much larger than the interatomic distances, a macroscopic approach is in general sufficient to describe the interaction between the impinging electrons and the excited vibrations. In this so-called dielectric approximation, the basic input for computing the EELS spectrum of a multilayered structure consists in the long-wavelength bulk dielectric functions of the successive layers that composes the target material, as summarized in sections 2 and 3 below. In section 4, a few technical details about the numerical techniques used are presented. The information about the input parameters is given in sections 5 and 6 and the results of a test run are given in section 7.

## 2. Theory of EELS in the specular geometry

Without going into any details (see e.g. ref. [3]), the theory of EELS provides us with the knowledge of the probability  $P(\omega) d\omega$  that an electron is inelastically scattered at the surface of the target material with an energy loss ( $\omega > 0$ ) or an energy gain ( $\omega < 0$ ) in the interval  $(\hbar\omega, \hbar\omega + \hbar d\omega)$ . In the dipolar-scattering regime that dominates the EELS spectrum in specular or near Bragg geometry, the energy-loss distribution  $P(\omega)$  can be computed using a semi-classical theory that proceeds in two sequential steps that we now summarize.

### 2.1. The classical loss spectrum (computer program EELS)

The first step of the semi-classical theory of EELS consists in evaluating the so-called classical spectrum  $P_{cl}(\omega)$ , which describes the loss spectrum of those electrons that have been inelastically scattered exactly once (single-scattering events) by surface excitations at zero temperature [2,9]:

$$P_{cl}(\omega) = \frac{e^2}{4\pi\epsilon_0\hbar v_{\perp}} \frac{2}{\pi^2} \times \int \int_D \frac{qv_{\perp}^3}{[(\mathbf{q} \cdot \mathbf{v}_{\parallel} - \omega)^2 + (qv_{\perp})^2]^2} \times \text{Im}[g(\mathbf{q}, \omega)] d^2q, \quad (1)$$

where  $\mathbf{v}_{\parallel}$  and  $v_{\perp}$  are the components of the electron velocity parallel and perpendicular to the surface, respectively, and  $g(\mathbf{q}, \omega)$  denotes the surface dielectric response of the target system to which we return below. In eq. (1),  $D$  is a domain of wave vectors  $\mathbf{q}$  of surface excitations with frequency  $\omega$ , which, according to the conservation of total energy and the momentum component parallel to the surface, scatter the electron towards the acceptance aperture of the energy analyzer. The analyzer must be centered around the specularly reflected electron beam for the theory to be valid.

In the program EELS described below, the acceptance aperture of the energy analyzer is assumed to be elliptical in shape, with half-acceptance

angles  $\phi_a$  and  $\phi_b$  measured along the two semi axes  $a$  and  $b$  of the elliptical slit, respectively oriented in the incidence plane and perpendicular to it (see fig. 1). In these conditions, the boundary of the domain  $D$  in eq. (1) is an ellipse whose equation valid for small  $\phi_a$  and  $\phi_b$  angles writes

$$(q_x v_{\parallel} - \omega)^2 + [q_x^2 + (\phi_a/\phi_b)^2 q_y^2] v_{\perp}^2 = (\omega \cos \theta)^2 \left[ 1 + \left( \frac{2E_0 \phi_a}{\hbar \omega} \right)^2 \right], \quad (2)$$

where  $E_0$  and  $\theta$  are the electron kinetic energy and incidence angle with respect to the outward normal at the surface,  $q_x$  and  $q_y$  are the Cartesian components of the surface wave vectors  $\mathbf{q}$  measured along directions parallel to  $\mathbf{v}_{\parallel}$  and perpendicular to it, respectively (see fig. 1). In usual spectrometers, the analyzer presents either a circular aperture or a rectangular slit, depending on the apparatus [10]. A rectangular slit will be approximated by an ellipse with opening angles  $\phi_a$  and  $\phi_b$  proportional to the width and the length of the slit, whereas a circular detector simply implies  $\phi_a = \phi_b$ .

### 2.2. The full loss probability (computer program BOSSON)

Multiple-scattering energy losses and gains for an arbitrary target temperature are accounted for through a thermodynamic average of boson-like surface excitations, which are viewed as quantum-mechanical harmonic oscillators driven by the Coulomb force exerted by a probing electron traveling along its classical trajectory [2]. The important result of this second step of the semi-classical theory is that the characteristic function  $F(\tau)$  of the energy-loss probability  $P(\omega)$ , i.e. its Fourier transform, only demands the 0-K classical spectrum:

$$F(\tau) \equiv \int_0^{\infty} P(\omega) \exp(-i\omega\tau) d\omega = \exp \left\{ - \int_0^{\infty} \coth \left( \frac{\hbar\omega'}{2k_B T} \right) P_{cl}(\omega') \times [1 - \cos(\omega'\tau)] d\omega' - i \int_0^{\infty} P_{cl}(\omega') \sin(\omega'\tau) d\omega' \right\}, \quad (3)$$

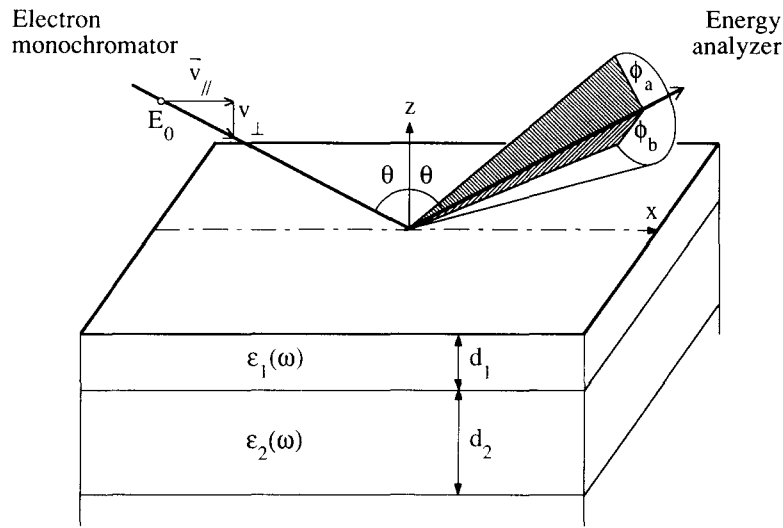


Fig. 1. Principles of high-resolution EELS experiment in specular geometry: a beam of mono-energetic electrons with primary energy  $E_0$  is incident upon the surface of a target. The impinging particles, through their Coulomb interactions with the ions or the electron gas of the target, exchange momentum and energy with long-wavelength charge oscillations that develop at the surface of the medium. The energy spectrum of the scattered electrons received by the spectrometer is analyzed. In the computer program described below, the entrance slit of the energy analyzer is an ellipse having its semi axes  $a$  and  $b$  respectively in the incidence ( $x, z$ ) plane and parallel to the surface of the target;  $\phi_a$  and  $\phi_b$  are the angles sustained by the two semi-axes  $a$  and  $b$ , respectively, of the elliptical slit. The target system can be composed of an arbitrary stacking of dielectric layers.

where  $k_B$  is the Boltzmann constant. The energy-loss spectrum, which is normalized to one at any target temperature  $T$ , follows by inverse Fourier transform of  $F(\tau)$ .

Considering as an illustrative example the ideal case of a sole, undamped surface excitation,  $P_{cl}(\omega)$  would be composed of a single Dirac delta peak  $A_{cl}\delta(\omega - \omega_s)$  at the frequency  $\omega_s$  of the surface mode. The full loss spectrum generated by the back-Fourier transform of eq. (3) in that simple case would be an infinite series  $\sum_{n=-\infty}^{+\infty} A_n \delta(\omega - n\omega_s)$  of delta peaks located at all the integer multiples of the fundamental frequency  $\omega_s$  and corresponding to emissions and absorptions of an arbitrary integer number of quanta  $\hbar\omega_s$ . At zero temperature, the amplitudes of the gain peaks ( $n < 0$ ) vanish and the amplitudes of the loss peaks follow a Poisson statistics:  $A_n = \exp(-A_{cl}) A_{cl}^n / n!$  ( $n \geq 0$ ). At non-zero temperature, the amplitudes  $A_n$  of the gain and loss peaks deviate from the Poisson law [11] according to a statistical distribution already considered in 1908 by the Swedish astronomer Charlier [12] in a very different context.

In more realistic situations, the loss probability  $P(\omega)$  must be computed numerically. Quantitative comparisons between experimental data and the theoretical energy-loss distribution require taking into account the limited energy resolution of the spectrometer. This experimental limitation can be simulated by convoluting  $P(\omega)$  with a model of the instrumental response function  $R(\omega)$ . This operation is best performed in Fourier space, by multiplying the characteristic function  $F(\tau)$  by the Fourier transform  $\Delta(\tau)$  of the broadening function  $R(\omega)$  before Fourier-transforming the result so as to obtain the convoluted loss distribution:

$$P(\omega) = \frac{1}{2\pi} \int_{-\infty}^{+\infty} \Delta(\tau) F(\tau) \exp(+i\omega\tau) d\tau. \quad (4)$$

### 3. Surface dielectric response of a multilayered target

The classical loss spectrum (1) has been formulated in terms of the surface dielectric response

$g(\mathbf{q}, \omega)$  [13] of the target material to an external electric field having the form of a plane wave with frequency  $\omega$  and wave vector  $\mathbf{q}$  parallel to the surface. For the short wave vectors selected by the energy analyzer in a specular EELS experiment, it is generally sufficient to approximate  $g(\mathbf{q}, \omega)$  by its expression deduced from electrostatics. For an arbitrary plane-stratified medium,  $g(\mathbf{q}, \omega)$  can then be cast into a form

$$g(\mathbf{q}, \omega) = \frac{\xi(\mathbf{q}, \omega) - 1}{\xi(\mathbf{q}, \omega) + 1} \quad (5)$$

that generalizes the expression  $[\epsilon(\omega) - 1]/[\epsilon(\omega) + 1]$  valid for a semi-infinite, homogeneous isotropic crystal with long-wavelength, bulk dielectric function  $\epsilon(\omega)$ . In the macroscopic limit, the surface dielectric function  $\xi(\mathbf{q}, \omega)$  of a multilayered system can be expressed in terms of the dielectric functions  $\epsilon_1(\omega), \epsilon_2(\omega), \dots$  of the successive layers (fig. 1). For the case of a multilayer made from isotropic materials,  $\xi$  is the continued fraction [14]

$$\xi(\mathbf{q}, \omega) = a_1 - \frac{b_1^2}{a_1 + a_2 - \frac{b_2^2}{a_2 + \dots}}, \quad (6)$$

with coefficients  $a_j = \epsilon_j(\omega)/\tanh(qd_j)$  and  $b_j = \epsilon_j(\omega)/\sinh(qd_j)$  where  $d_j$  is the thickness of the  $j$ th layer. Under the assumption of isotropic materials,  $\xi(\mathbf{q}, \omega)$  no longer depends on the direction of the wave vector  $\mathbf{q}$  but only on its modulus  $q$ .

When the  $N$ th layer of the target is a thick substrate, the related coefficient  $a_N$  identifies with the dielectric function  $\epsilon_N(\omega)$  of the substrate whereas  $b_N$  vanishes. The continued fraction (6) then terminates at the  $N$ th level (possibly  $N = 1$  for the particular case of a homogeneous semi-infinite material) and it can be evaluated using a backward algorithm. Generalization to the case of a non-isotropic substrate can be found in ref. [15]. When the thick substrate is a uniaxial crystal with its axis normal to the surface of the target, in particular, one obtains  $a_N = \sqrt{\epsilon_{\perp}(\omega)\epsilon_{\parallel}(\omega)}$ , where  $\epsilon_{\perp}$  and  $\epsilon_{\parallel}$  are the two principal components of the substrate dielectric tensor, and the surface dielectric response of the system is still isotropic with respect to the direction of  $\mathbf{q}$ . The program

described below allows one to consider this situation, with the restriction however that the  $N - 1$  layers possibly deposited onto the substrate be isotropic materials.

The surface dielectric function  $\xi(\mathbf{q}, \omega)$  of a superlattice, with many identical repetitions of a sequence of  $p$  layers, is more conveniently obtained by considering the limit of an infinite number of periods. The continued-fraction expression (6) itself becomes periodic if  $p \geq 2$  and its limit is easily obtained by solving a quadratic equation [16]. From this limit, a backward algorithm can be used here again to evaluate  $\xi(\mathbf{q}, \omega)$  when several additional layers are deposited onto the superlattice.

Equation (6) still demands analytical expressions for the frequency dependence of the dielectric functions of the individual layers. It will be assumed that the thickness of the layers is large enough at the atomic scale to characterize their responses by bulk dielectric functions. In the infra-red domain, it is then generally legitimate to represent the dielectric function of a given layer by a sum of  $n$  Lorentzian terms,

$$\epsilon(\omega) = \epsilon(\infty) + \sum_{k=1}^n \frac{Q_k \omega_{\text{TO},k}^2}{\omega_{\text{TO},k}^2 - \omega^2 - i\gamma_k \omega}, \quad (7)$$

where  $\omega_{\text{TO},k}$  denote transverse-optical phonon frequencies, with strenghts  $Q_k$  and damping frequencies  $\gamma_k$  as deduced from infra-red data and  $\epsilon(\infty)$  is the high-frequency dielectric constant. In certain cases (doped semi-conductors for instance), infra-red reflectivity measurements are best reproduced when a Drude contribution

$$\frac{-\omega_p^2}{\omega^2 + i\gamma\omega} \quad (8)$$

is added to the right-hand side of eq. (7). Here  $\omega_p$  is the bulk plasmon frequency of the charge carriers and the Ohmic damping frequency  $\gamma$  is the reciprocal of the free-carrier relaxation time  $\tau$ .

#### 4. Numerical techniques

In this section, we present a few technical details about the numerical techniques used to

calculate the EELS spectrum. For a given energy loss  $\hbar\omega$ , the two-dimensional  $\mathbf{q}$ -space integration in the expression (1) of  $P_{\text{cl}}(\omega)$  is performed in polar coordinates. With the explicit assumption of an isotropic target, the integral over the polar angle  $\varphi$  of  $\mathbf{q}$  can be performed analytically, leading to an expression that is more easily handled in complex arithmetics (see the appendix in ref. [14]). The lower and upper limits for the integration over  $\varphi$  for a given modulus  $q$  of  $\mathbf{q}$  are obtained by looking for the intersections of a circle of radius  $q$  and the ellipse given by eq. (2). This problem is not always a well-conditioned one: for that reason, we prefer using 64-bit arithmetics on a IBM computer rather than the single-precision operations. There is nevertheless a substantial benefit in so-doing as only a one-dimensional numerical integration over  $q$  is left out. The latter is performed using a Newton–Cotes 8-panel adaptative quadrature routine described in ref. [17].

For the particular important case of a homogeneous thick target with dielectric function  $\epsilon(\omega)$ , eq. (1) can be factorized into

$$P_{\text{cl}}(\omega) = \frac{e^2}{4\pi\epsilon_0\hbar v_{\perp}} w_{\theta} \left( \frac{\hbar\omega}{2E_0\phi_a} \right) \text{Im} \left[ \frac{\epsilon(\omega) - 1}{\epsilon(\omega) + 1} \right] / \omega, \quad (9)$$

where  $w_{\theta}$  denotes the  $\mathbf{q}$ -integral of eq. (1) without the factor  $\text{Im}[g]$ , which no longer depends on  $q$  in the present situation. This integral does not depend on the target material; it is a function of the variable  $X = \hbar\omega/2E_0\phi_a$ , which monotonously decreases from 1 for  $X = 0$  to 0 when  $X$  approaches infinity. The integral  $w_{\theta}(X)$  also depends on the incidence angle  $\theta$  and on the ratio  $\phi_b/\phi_a$  of the two acceptance angles of the elliptical slit of the spectrometer. In the program EELS, a rational approximation for  $w_{\theta}(X)$  is constructed when the target is a thick homogeneous substrate: with the help of such an analytical, though approximate expression, the time required to compute the loss spectrum is considerably reduced. The expression used for  $w_{\theta}(X)$  is

$$w_{\theta}(X) \approx \frac{1}{(1 + \alpha X)^2} \frac{1 + \beta X + C_1 X^2}{1 + \beta X + C_2 X^2}. \quad (10)$$

The coefficients  $\alpha$ ,  $C_1$  and  $C_2$  are fitted to the exact asymptotic laws of  $w_{\theta}(X)$  for small and large values of  $X$ , leading to

$$\alpha = (2/\pi)^2 \int_0^{\pi/2} (1 - n \cos^2 \psi)^{1/2} \times (1 - \cos^2 \theta \sin^2 \psi)^{1/2} d\psi, \quad (11)$$

$$C_1 = (2/\pi)(\phi_b/\phi_a) \sin \theta \alpha^2 C_2,$$

$$C_2 = \frac{3\alpha^2}{1 - (2/\pi)(\phi_b/\phi_a) \sin \theta \alpha^2}. \quad (12)$$

In eq. (11),  $n = 1 - (\phi_a/\phi_b)^2$ . The expression obtained for  $\alpha$  is a non-standard (except for  $n = 0$ ) elliptic integral that can be evaluated numerically with a high degree of precision. The values of  $C_1$  and  $C_2$  follow from eq. (12). The remaining parameter  $\beta$  in eq. (10) is adjusted numerically so as to best reproduce numerical values of  $w_{\theta}$  computed for a few abscissae in the range of interest of the energy losses. The absolute accuracy obtained by using a rational approximation for  $w_{\theta}$  is better than  $10^{-3}$  in most applications. Selected coefficient values are reproduced in table 1.

Consider now the calculation of the full loss distribution  $P(\omega)$ . The expression (3) for the characteristic function  $F(\tau)$  demands evaluating sine and cosine-like integral transforms. The latter is transformed into a sine integral by a straightforward integration by parts,

$$\int_0^{\infty} \coth \left( \frac{\hbar\omega'}{2k_B T} \right) P_{\text{cl}}(\omega') [1 - \cos(\omega'\tau)] d\omega' = \tau \int_0^{\infty} G(\omega') \sin(\omega'\tau) d\omega', \quad (13)$$

where

$$G(\omega') = \int_{\omega'}^{\infty} \coth \left( \frac{\hbar\omega}{2k_B T} \right) P_{\text{cl}}(\omega) d\omega. \quad (14)$$

For the purpose of computing  $F(\tau)$ , the classical loss spectrum  $P_{\text{cl}}(\omega)$  is evaluated on a regular mesh of frequencies  $\omega_i$  with a step size  $\delta\omega$  specified by the user. In a given panel  $(\omega_{i-1/2}, \omega_{i+1/2})$ ,  $P_{\text{cl}}(\omega)$  is approximated by a rectangle with height  $P_{\text{cl}}(\omega_i)$ . To validate this approximation, the step size  $\delta\omega$  must be taken smaller than the damping

Table 1

Coefficients of the expression (10) useful for computing the classical loss spectrum of a homogeneous thick target for an energy analyzer presenting a circular aperture ( $\phi_b/\phi_a = 1$ ) or a thin "horizontal" slit ( $\phi_b/\phi_a = 10$ ). The coefficient  $\beta$  has been optimized for  $X$  in the interval (0,1), leading to a root mean square deviation  $\epsilon$  given in the last column of the table

$\phi_b/\phi_a$	$\theta(^{\circ})$	$\alpha$	$C_1$	$C_2$	$\beta$	$\epsilon$
1	0	0.6366	0.0000	1.2159	0.1570	$2.5 \cdot 10^{-4}$
	5	0.6354	0.0278	1.2390	0.1383	$3.3 \cdot 10^{-4}$
	10	0.6318	0.0553	1.2528	0.1331	$3.6 \cdot 10^{-4}$
	15	0.6258	0.0811	1.2560	0.1419	$3.4 \cdot 10^{-4}$
	20	0.6176	0.1036	1.2478	0.1650	$2.6 \cdot 10^{-4}$
	25	0.6072	0.1218	1.2277	0.2016	$1.6 \cdot 10^{-4}$
	30	0.5947	0.1346	1.1958	0.2502	$5.8 \cdot 10^{-5}$
	35	0.5805	0.1418	1.1527	0.3075	$1.5 \cdot 10^{-4}$
	40	0.5646	0.1435	1.0999	0.3687	$2.6 \cdot 10^{-4}$
	45	0.5474	0.1402	1.0391	0.4267	$3.4 \cdot 10^{-4}$
	50	0.5291	0.1328	0.9727	0.4701	$3.3 \cdot 10^{-4}$
	55	0.5101	0.1226	0.9033	0.4859	$2.2 \cdot 10^{-4}$
	60	0.4908	0.1107	0.8334	0.4657	$7.1 \cdot 10^{-5}$
	65	0.4717	0.0983	0.7657	0.4090	$1.5 \cdot 10^{-4}$
	70	0.4533	0.0864	0.7027	0.3231	$2.3 \cdot 10^{-4}$
	75	0.4363	0.0757	0.6466	0.2209	$1.6 \cdot 10^{-4}$
	80	0.4215	0.0668	0.5999	0.1180	$1.8 \cdot 10^{-4}$
	85	0.4104	0.0604	0.5658	0.0318	$5.3 \cdot 10^{-4}$
10	0	0.4118	0.0000	0.5087	0.8012	$7.6 \cdot 10^{-4}$
	5	0.4107	0.0523	0.5584	0.7617	$6.9 \cdot 10^{-4}$
	10	0.4077	0.1122	0.6108	0.7286	$6.1 \cdot 10^{-4}$
	15	0.4026	0.1771	0.6633	0.7038	$5.5 \cdot 10^{-4}$
	20	0.3955	0.2425	0.7118	0.6905	$5.0 \cdot 10^{-4}$
	25	0.3866	0.3017	0.7502	0.6931	$4.7 \cdot 10^{-4}$
	30	0.3760	0.3471	0.7712	0.7161	$4.6 \cdot 10^{-4}$
	35	0.3638	0.3712	0.7682	0.7613	$4.7 \cdot 10^{-4}$
	40	0.3501	0.3701	0.7379	0.8243	$4.8 \cdot 10^{-4}$
	45	0.3352	0.3452	0.6824	0.8905	$4.7 \cdot 10^{-4}$
	50	0.3194	0.3029	0.6089	0.9296	$4.0 \cdot 10^{-4}$
	55	0.3028	0.2521	0.5272	0.9018	$2.5 \cdot 10^{-4}$
	60	0.2859	0.2011	0.4463	0.7828	$6.6 \cdot 10^{-5}$
	65	0.2690	0.1555	0.3726	0.5810	$1.4 \cdot 10^{-4}$
	70	0.2526	0.1181	0.3095	0.3339	$1.7 \cdot 10^{-4}$
	75	0.2373	0.0894	0.2583	0.0873	$1.6 \cdot 10^{-4}$
	80	0.2239	0.0689	0.2192	-0.1237	$6.1 \cdot 10^{-4}$
	85	0.2136	0.0557	0.1926	-0.2771	$1.3 \cdot 10^{-3}$

frequencies  $\gamma_k$  of the dielectric functions (7). The same rectangle approximation is used to represent the function  $G(\omega')$  introduced in eq. (14) and the two terms into the argument of the exponential in the expression (3) of  $F(\tau)$  can then be converted into discrete sums which can be computed by a fast-Fourier transform (FFT) technique for discrete values of  $\tau$  in the interval  $(0, 2\pi/\delta\omega)$ . The characteristic function  $F(\tau)$  is next multiplied by the Fourier transform  $\Delta(\tau)$  of a suitable instrumental response (see eq. (4)) and  $P(\omega)$  follows by

back-Fourier transform which, here again, is evaluated by a FFT technique. Note that the width of the instrumental response must be larger than the frequency step size  $\delta\omega$  to guarantee a fast decay of the product  $\Delta(\tau)F(\tau)$  when  $\tau$  approaches its maximum value  $2\pi/\delta\omega$ .

## 5. Structure of the program EELS

The program EELS is aimed at computing the classical loss spectrum given by eq. (1) for an

Table 2

The input data for the file EELSIN (unit = 11)

Format	Variable	Comment
<i>Spectrometer parameters</i>		
*	EO	Electron primary energy $E_0$ (eV)
*	THETA	Incidence angle $\theta$ of the electrons ( $^\circ$ ), $0 \leq \theta \leq 90^\circ - \phi_a$
*	PHIA	Half-acceptance angle $\phi_a$ sustained by the vertical (in the incidence plane) semi-axis of the elliptical slit of the spectrometer ( $^\circ$ ) (see fig. 1)
*	PHIB	Half-acceptance angle $\phi_b$ sustained by the horizontal (parallel to the target surface) semi-axis of the elliptical slit of the spectrometer ( $^\circ$ ) (see fig. 1)
*	WMIN	Lower frequency value $\omega$ for ( $\text{cm}^{-1}$ ) for the computation of $P_{cl}(\omega)$ , WMIN $> 0$
*	WMAX	Upper frequency value $\omega$ ( $\text{cm}^{-1}$ )
*	DW	Step for the grid of equally-spaced frequencies ( $\text{cm}^{-1}$ )
<i>Target specification</i>		
A72	COMMEN(1)	Two lines of comments, for user convenience, the first of which will be copied in the output file EELSOU as a title
A72	COMMEN(2)	
*	N, NPER	The number N of layers, with the possibility of reproducing periodically the NPER ( $\leq N$ ) last layers. When NPER $= \pm 1$ , the Nth layer is assumed to be a thick substrate made either from an isotropic material (NPER $= +1$ ) or a uniaxial crystal (NPER $= -1$ ) with its axis perpendicular to the surface of the target. If N = 0, the rest of the input file is not used and the program switches to a user-supplied external routine USURLO for computing the surface loss function $\text{Im}[g(q, \omega)]$ (see eq. 1)
<i>Dielectric functions (N such blocks of data for the N layers)</i>		
A10,E15.5	NAME(j), THICK(j)	A character *10 string identifying the material which the jth layer is made from and the thickness $d_j$ of that layer ( $\text{\AA}$ ). With NPER $= \pm 1$ , the thickness of the bottom layer ( $j = N$ ) is assumed infinite; the corresponding variable THICK(N) is not used and may be entered as any large number
*	EPSINF(j), NOS(j)	The high-frequency dielectric constant $\epsilon(\infty)$ and the number of oscillators, including a possible Drude contribution, in the expression (eqs. (7) and (8)) of the dielectric function for layer j. NOS(j) can be zero in which case $\epsilon(\omega) \equiv \epsilon(\infty)$
*	WTO(k, j), Q(k, j), LAM(k, j)	NOS(j) such lines giving for the kth oscillator in the expression (7) of the dielectric function: the resonant frequency $\omega_{\text{TO},k}$ (in $\text{cm}^{-1}$ ), the strength $Q_k$ ( $\geq 0$ ) and the damping constant $\lambda_k = \gamma_k / \omega_{\text{TO},k}$ in units of $\omega_{\text{TO},k}$ . For a Drude contribution (8), enter $Q(k, j) = -1$ in which case WTO(k, j) is interpreted as a bulk plasmon frequency $\omega_p$
<i>Oscillator parameters for the second principal component of the dielectric tensor of the Nth layer when NPER = -1: uniaxial thick substrate</i>		
*	EPSINF(N+1), NOS(N+1)	Same meaning as here above for $\epsilon_{\parallel}(\omega)$ when the substrate is a uniaxial crystal (see section 3), the corresponding parameters for $\epsilon_{\perp}(\omega)$ having been entered in EPSINF(N), NOS(N)
*	WTO(k, N+1), Q(k, N+1), GAM(k, N+1)	NOS(N+1) such lines, with the same meaning as here above, for $\epsilon_{\parallel}(\omega)$ when the substrate is a uniaxial crystal (NPER = -1)
<i>Optional control variable (this last line of the input may be omitted)</i>		
A10	CONTRL	When the character *10 variable CONTRL is equal to "IMAGE", shortening of the interaction-time arising from the image attraction of the electron is accounted for as explained in section 5

arbitrary multilayered target. The output (file EELSOU, unit = 12) consists in a table of values of  $P_{cl}(\omega)$  computed on a regular mesh of frequen-

cies  $\omega_i$  in the interval  $(\omega_{\min}, \omega_{\max})$  with a step size  $\delta\omega$ , both specified by the user in an input file called EELSIN (unit = 11). The input file contains



in addition the electron primary energy  $E_0$ , the incidence angle  $\theta$  and the half-aperture angles  $\phi_a$  and  $\phi_b$  of the energy analyzer (see fig. 1). The rest of the input file, described in table 2, contains target specifications and oscillator parameters to be used for computing the dielectric functions of the individual layers.

The most general system that can be handled is composed of  $N$  layers, with the possibility of reproducing periodically the last  $p$  layers ( $1 \leq p \leq N$ ) so as to deal with superlattices. This includes as particular cases the following systems (note the use of the parameters  $N$  and  $p$  to distinguish between the different cases):

- (a) a thick (semi-infinite) homogeneous crystal ( $N = p = 1$ );
- (b) a single film or a multilayered medium deposited onto a thick substrate ( $N \geq p = 1$ ); in that case, the  $N$ th layer is the substrate;
- (c) a superlattice with an arbitrary number of layers per period ( $N \geq p \geq 2$ ).

For instance, a system like AlAs/GaAs with  $N = 2$  layers can be considered either as a superlattice ( $p = 2$ ) or an AlAs film onto a semi-infinite GaAs substrate ( $p = 1$ ). When  $N = p = 1$ , the approximate, rational expression (10) of  $w_\theta$  is used for computing  $P_{cl}(\omega)$ , leading to a considerable reduction of the computing time. When  $p = 1$ , the thick substrate may be a uniaxial crystal as explained in section 3 (this option works for all values of  $N \geq 1$ ). By convention it suffices to enter  $p = -1$  to tell the program that the substrate is a uniaxial material; two sets of oscillator parameters for the two principal components  $\epsilon_\perp(\omega)$  and  $\epsilon_\parallel(\omega)$  of the dielectric tensor of the  $N$ th layer must then be provided (more details are given in table 2).

The surface loss function  $\text{Im}[g(q, \omega)]$  of the multilayered target (5) is evaluated in complex arithmetics using the continued-fraction expression (6) for  $\xi$  (external functions SURLOS). The dielectric functions of the individual layers are computed by eqs. (7) and (8) (subroutine SETEPS) from a table of oscillator parameters contained in the input file (see table 2). Undamped oscillators may give rise to numerical problems; it is therefore recommended to use non-zero damping frequencies  $\gamma_k$  (1% of the resonant frequencies  $\omega_{TO,k}$  for instance, if no known data is available).

By entering an extra line of input with the string "IMAGE" (see table 2), possibility exists to take into account, at least approximately, the acceleration of the electrons associated with the image potential. The image acceleration, which is not included in the expression (1) of the classical loss spectrum, is responsible for shortening the interaction time of the electrons with the long-wavelength surface excitations of the target. The integrand in the expression (1) of  $P_{cl}$  is corrected on request for the shortening of the interaction time [18] arising from the attraction of the electron by a quasi-instantaneous image with charge  $-\beta e$  where, for a thick homogeneous target,  $\beta = [\epsilon(\infty) - 1]/[\epsilon(\infty) + 1]$ . For a multilayered system, the screening factor  $\beta$  is evaluated from the high-frequency dielectric constant of the top-most layer. The image attraction, which has important effects at grazing incidences, can usually be neglected when  $\theta < 60^\circ$ .

By entering a zero value for the number  $N$  of layers in line 10 of the input file (table 2), the program switches to a user-supplied expression of the surface loss function  $\text{Im}[g]$  instead of the continued fraction [6] when evaluating the classical loss spectrum. The actual surface loss function of the target system can be coded in a external function USURLO(Q, W) which returns  $\text{Im}[g(q, \omega)]$  (dimensionless) for given  $q$  and  $\omega$ . The two input arguments Q and W denote, respectively, the modulus  $q$  of the surface wave vector (in  $\text{\AA}^{-1}$ ) and the frequency  $\omega$  (in  $\text{cm}^{-1}$ ).

## 6. Structure of the program BOSON

The second step of the semi-classical theory summarized in section 2 is performed by the program BOSON. This program uses as an input the table of values of the classical spectrum  $P_{cl}(\omega)$  generated by the program EELS in the file EELSOU (unit = 12). The other input parameters must be specified in another input file, called BOSIN (unit = 13), whose structure is described in table 3. As explained in section 4, all the Fourier integrals required are performed using a FFT technique. In order to save time, a radix-two form of the FFT algorithm is applied throughout.

Table 3

The input data for the file BOSIN (unit = 13)

Format	Variable	Comment
*	T	Target temperature (K)
*	WIDTH	The width of the instrumental response ( $\text{cm}^{-1}$ ) of the spectrometer. WIDTH can be estimated by measuring the full width at half maximum of the experimental elastic peak
*	GAUSS	The relative weight of the Gaussian term in the Gaussian–Lorentzian linear combination modeling the instrumental response $R(\omega)$ of the spectrometer. When $\text{GAUSS} < 0$ or $\text{GAUSS} > 1$ , the program switches to a user-supplied expression of $R(\omega)$ (external function RESPON)
*	ASYM	ASYM controls the asymmetry of the Lorentzian component (see section 6) of the Gaussian–Lorentzian expression used by default as a model for the instrumental response ( $-1 \leq \text{ASYM} \leq +1$ )
*	EMIN	Lower value of the energy losses $\hbar\omega$ ( $\text{cm}^{-1}$ ). A negative value of EMIN allows one to explore the gain region of the EELS loss distribution $P(\omega)$
*	EMAX	Upper value of the energy losses $\hbar\omega$ ( $\text{cm}^{-1}$ )

The frequency interval explored by the program EELS is enlarged by raising the number of grid points to a power of 2, while keeping the step size  $\delta\omega$  that was used for computing the classical loss spectrum, and  $P_{\text{cl}}(\omega)$  is set to zero for those grid points that are outside the tabulated interval ( $\omega_{\text{min}}, \omega_{\text{max}}$ ) contained in the file EELSOU.

The instrumental response  $R(\omega)$  of the spectrometer used to broaden the theoretical loss spectrum  $P(\omega)$  according to eq. (4) can be any normalized linear combination of a Gaussian function and a Lorentzian function, both with the same width (FWHM). Alternatively,  $R(\omega)$  can be computed from a user-supplied expression coded in an external function called RESPON (W,WIDTH). The two input arguments W and WIDTH are the frequency  $\omega$  in  $\text{cm}^{-1}$  (equal to the energy loss or gain, depending on the sign of  $\omega$ , divided by  $\hbar$ ) and the width of the broadening function ( $\text{cm}^{-1}$ ) as read in the file BOSIN. The program switches to the user-supplied response whenever the parameter GAUSS in line 3 of the input file BOSIN is smaller than 0 or larger than 1. The Fourier transform  $\Delta(\tau)$  of the instrumental response is then computed numerically.

With  $0 \leq \text{GAUSS} < 1$ , the Lorentzian component of the instrumental response used by default can be made asymmetric. More clearly stated, this component is built from two halves of Lorentzian functions, one with half width  $\gamma_1$  in the energy-gain

region ( $\omega < 0$ ) and the other with half width  $\gamma_2$  in the energy-loss region ( $\omega > 0$ ). By construction  $\gamma_2 + \gamma_1$  is equal to the width of the instrumental response. The asymmetry (parameter ASYM in the input file) of the Lorentzian component is defined as the ratio  $(\gamma_2 - \gamma_1)/(\gamma_2 + \gamma_1)$ , which vanishes for a symmetric function ( $\gamma_1 = \gamma_2$ ).

The output of the program is written in a file called BOSOU (unit = 14), where the full EELS spectrum is tabulated from EMIN to EMAX (input values) with equidistant steps equal to the one  $\delta\omega$  used for the input table of  $P_{\text{cl}}$  or, possibly, to an integer multiple of  $\delta\omega$  not larger than (1/20)-th of the resolution parameter WIDTH.

## 7. Test run

The input and output files of the test run correspond to the EELS spectrum of an GaAs/AlGaAs superlattice described in ref. [7]. The sample consists of a repetition of alternate GaAs and  $\text{Al}_{0.3}\text{Ga}_{0.7}\text{As}$  layers, each of them is 100 Å thick, except for the topmost GaAs layer whose thickness was reduced to an estimate of 70 Å while sputter cleaning the surface. The target is therefore considered as a GaAs 70 Å overlayer onto a AlGaAs/GaAs (100 Å/100 Å) semi-infinite superlattice ( $N = 3$ ,  $p = 2$ ). The parameters of the dielectric functions for GaAs (one oscilla-

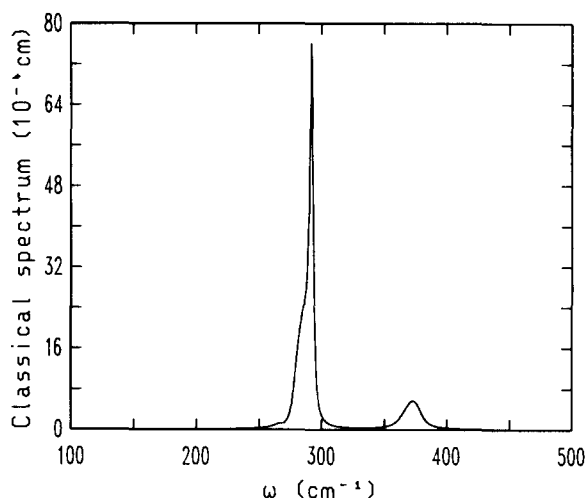


Fig. 2. Classical loss spectrum  $P_{cl}(\omega)$  of a GaAs/AlGaAs superlattice generated by the program EELS in the test run described in the text.

tor) and  $\text{Al}_{0.3}\text{Ga}_{0.7}\text{As}$  (two oscillators) are taken from published infra-red data. The classical loss spectrum (see fig. 2) has been computed with a primary electron energy of 6.1 eV and an incidence angle of  $45^\circ$ , the spectrometer acceptance angles are  $\phi_a = \phi_b = 1.8^\circ$  (circular aperture). Acceleration of the electrons by their image charges is ignored. The output of the program EELS consists of a table of values of  $P_{cl}(\omega)$  from

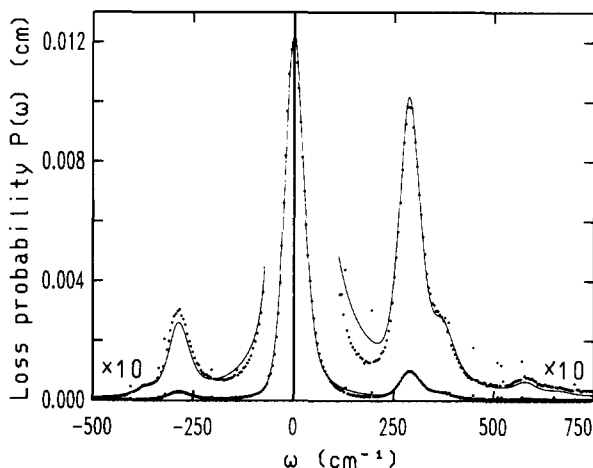


Fig. 3. Full loss probability  $P(\omega)$  (solid line) generated by the program BOSON for the GaAs/AlGaAs superlattice considered in the test run. For comparison, the corresponding experimental spectrum [7] is shown by dots.

$\omega_{\min} = 100$  to  $\omega_{\max} = 500 \text{ cm}^{-1}$  with a step size  $\delta\omega = 2 \text{ cm}^{-1}$ .

The full loss probability  $P(\omega)$  obtained by the program BOSON is shown in fig. 3, where it is compared with an experimental spectrum. The instrumental response function  $R(\omega)$  used to broaden the theoretical EELS spectrum is a combination of a Gaussian and a Lorentzian with equal weights (GAUSS = 0.5). This parameter together with the width ( $57 \text{ cm}^{-1}$ ) of  $R(\omega)$  and the asymmetry parameter of the Lorentzian component (ASYM = 0.3) have been adjusted to the shape of the experimental elastic peak around  $\omega = 0$ .

### Acknowledgements

This work was funded by the Interuniversity Research Program (Pôles d'Attraction Interuniversitaires) on Interface Sciences initiated by the Belgian State Prime Minister Office (Science Policy Programming). The authors are also grateful to Paul A. Thiry for helpful suggestions and stimulating discussions. This work has benefited from the Namur Scientific Facility, a common project between the National Fund for Scientific Research of Belgium, IBM-Belgium and the Facultés Universitaires Notre-Dame de la Paix in Namur.

### References

- [1] H. Ibach, Phys. Rev. Lett. 24 (1970) 1416.
- [2] A.A. Lucas and M. Sunjic, Phys. Rev. Lett. 26 (1971) 229.  
M. Sunjic and A.A. Lucas, Phys. Rev. B 3 (1971) 719.
- [3] A.A. Lucas, J.-P. Vigneron, Ph. Lambin, P.A. Thiry, M. Liehr, J.-J. Pireaux and R. Caudano, Int. J. Quantum Chem.: Quantum Chem. Symp. 19 (1986) 687.
- [4] P.A. Thiry, M. Liehr, J.-J. Pireaux and R. Caudano, Phys. Rev. B 29 (1984) 4824.
- [5] Z.J. Gray-Grychowski, R.G. Egdell, B.A. Joyce, R.A. Stradling and K. Woodbridge, Surf. Sci. 186 (1987) 482.
- [6] M. Liehr, P.A. Thiry, J.-J. Pireaux and R. Caudano, Phys. Rev. B 34 (1986) 7471.
- [7] Ph. Lambin, J.-P. Vigneron, A.A. Lucas, P.A. Thiry, M. Liehr, J.-J. Pireaux, R. Caudano and T.J. Kuech, Phys. Rev. Lett. 56 (1986) 1842.
- [8] A. Förster, J.M. Layet and A. Lüth, Appl. Surf. Sci. 41/42 (1989) 306.

- [9] E. Evans and D.L. Mills, *Phys. Rev. B* 5 (1972) 4126.
- [10] D. Roy and J.D. Carette, in: *Electron Spectroscopy for Surface Analysis*, ed. H. Ibach (Springer, Berlin, 1977).
- [11] Ph. Lambin, J.-P. Vigneron and A.A. Lucas, *J. Electron Spectrosc. Relat. Phenom.* 39 (1986) 59.
- [12] C.V.L. Charlier, *Ark. Mat. Astron. Fys.* 4 (13) (1908) 1.
- [13] B.N.J. Persson and J.E. Demuth, *Phys. Rev. B* 30 (1984) 5968.
- [14] Ph. Lambin, J.-V. Vigneron and A.A. Lucas, *Phys. Rev. B* 32 (1985) 8203.
- [15] A.A. Lucas and J.-P. Vigneron, *Solid State Commun.* 49 (1984) 327.
- [16] H.S. Wall, *Analytic Theory of Continued Fractions* (Chelsea, New York, 1973).
- [17] G.E. Forsythe, M.A. Malcom and C.B. Moler, *Computer Methods for Numerical Computations* (Prentice-Hall, Englewood Cliffs, NJ, 1977) pp. 97–105.
- [18] Ph. Lambin, A.A. Lucas and J.-P. Vigneron, *Surf. Sci.* 182 (1987) 567.

**TEST RUN INPUT AND OUTPUT****File EELSIN, unit = 11**

```

6.1      E0
45.0     THETA
1.8      PHIA
1.8      PHIB
100.0    WMIN
500.0    WMAX
2.0      DW
GAAS 70.0 ( AL30GA70AS 100.0 GAAS 100.0 )

3      2
GAAS      0.70000D+02      N NPER
10.900    1      LAYER 1
269.20    2.0300      0.93000E-02
AL30GA70AS 0.10000D+03      LAYER 2
10.200    2
265.00    1.2400      0.27000E-01
361.00    0.93000      0.30000E-01
GAAS      0.10000D+03      LAYER 3
10.900    1
269.20    2.0300      0.93000E-02

```

**File EELSOU (shortened), unit = 12**

```

E0 = 6.10 THETA = 45.0 PHIA = 1.80 PHIB = 1.80
GAAS 70.0 ( AL30GA70AS 100.0 GAAS 100.0 )
0.1000000E+03 0.3389797E-05
0.1020000E+03 0.3414600E-05
0.1040000E+03 0.3440501E-05
0.1060000E+03 0.3467530E-05
0.1080000E+03 0.3495730E-05
0.1100000E+03 0.3525141E-05
0.1120000E+03 0.3555810E-05
0.1140000E+03 0.3587780E-05
0.1160000E+03 0.3621101E-05
0.1180000E+03 0.3655827E-05
0.1200000E+03 0.3692012E-05
.
.
.
0.4900000E+03 0.1256209E-05
0.4920000E+03 0.1210072E-05
0.4940000E+03 0.1166246E-05
0.4960000E+03 0.1124578E-05
0.4980000E+03 0.1084930E-05
0.5000000E+03 0.1047181E-05

```

**File BOSIN, unit = 13**

```

300.0    T
57.0     WIDTH
0.5      GAUSS
0.3      ASYM
-500.0    EMIN
750.0     EMAX

```

**File BOSOU (shortened), unit = 14**

E0 = 6.10 THETA = 45.0 PHIA = 1.80 PHIB = 1.80 T = 300.0 GAUSS = 0.50  
 GAAS 70.0 ( AL30GA70AS 100.0 GAAS 100.0 )

-0.5000000E+03	0.1041774E-04
-0.4980000E+03	0.1049992E-04
-0.4960000E+03	0.1058362E-04
-0.4940000E+03	0.1067086E-04
-0.4920000E+03	0.1076084E-04
-0.4900000E+03	0.1085463E-04
-0.4880000E+03	0.1095019E-04
-0.4860000E+03	0.1104833E-04
-0.4840000E+03	0.1115222E-04
-0.4820000E+03	0.1125614E-04
-0.4800000E+03	0.1136563E-04
.	.
.	.
0.7400000E+03	0.1824343E-04
0.7420000E+03	0.1807071E-04
0.7440000E+03	0.1790094E-04
0.7460000E+03	0.1773359E-04
0.7480000E+03	0.1756617E-04
0.7500000E+03	0.1740073E-04